Thermal damping width of the giant dipole resonance in hot nuclei

Nguyen Dinh Dang [1] and Fumihiko Sakata [2]
[1] *Cyclotron Laboratory, RIKEN, Wako, Saitama 351-01, Japan*
[2] *Department of Mathematical Sciences, Ibaraki University, Mito 310, Japan*
(Received 8 November 1996)

An approach describing the thermal damping width of the giant dipole resonance (GDR) in hot nuclei is presented. The GDR is generated by the ph excitations within the finite-temperature random-phase approximation (FTRPA), while its damping at finite temperature arises from irreversible coupling of ph configurations to the thermal pp and hh ones beyond the FTRPA. A semimicroscopic unification of the quantal spreading and thermal damping widths is undertaken within the framework of motional damping. The numerical calculations are performed, using a schematic model with equally degenerate equidistant shells for a hot nucleus of mass $A=112$ carrying no angular momentum. The results show that the total width of the GDR increases strongly as a function of the excitation energy up to $E^*\sim 120-130$ MeV, where it reaches a saturation value. The limiting temperature for the GDR in very hot nuclei is discussed. [S0556-2813(97)03806-5]

PACS number(s): 24.30.Cz, 21.60.Jz, 24.60.−k, 27.60.+j

I. INTRODUCTION

A great interest has been devoted to the properties of highly excited nuclei produced in heavy-ion fusion reactions during the last decade. Analyzing the decay pattern of these hot nuclei, the giant dipole resonance (GDR) built on compound nuclear states has been observed [1–8]. The experiments have shown that while centroid energy of the hot GDR is almost independent of excitation energy (or temperature T), its apparent width increases strongly as the excitation energy goes up, and saturates at around 130 MeV in Sn isotopes. This attractive phenomenon has become a real puzzle to be resolved for many theoretical studies in recent years (see [9] for an overview). Indeed, while most of theoretical approaches agree in reproducing the centroid energy of the GDR at $T\neq 0$, many of them are still in contradiction with each other in understanding the GDR width in hot nuclei. As an example we refer to two theoretical predictions in Refs. [10,11]. The former assumes a GDR width as the square root of a quadratic sum of three terms Γ_Q, $\Gamma_{0,\pm 1}$, and Γ_T in the adiabatic regime, where Γ_Q is temperature independent, $\Gamma_{0,\pm 1}$ is proportional to the nuclear spin in square, Γ_T is proportional to the square root of temperature, and the width saturation is explained as the saturation of the maximum spin $J_{\max}$. The latter proposes a continuously increasing width with temperature. The quite recent measurements in Ref. [12], however, have shown that, in order to reproduce the γ spectra from the hot GDR in ^{112}Sn, the increase of the width as a function of excitation energy (temperature) must be much more rapid than both of these predictions. It has also been pointed out in Ref. [12] that the point should be proved more clearly the role played by thermal and angular momentum effects in the low excitation energy region ($E^*\leqslant 200$ MeV). The exclusive measurements in Ref. [13] have shown a small increase of the total GDR width (by roughly 1.2 MeV) with increasing the angular momentum from spin 43 to spin 51 at $T\simeq 2$ MeV in Sn isotopes. This conclusion is reconfirmed in the recent measurements by Mattiuzzi *et al.* [14], where it has been shown clearly that the GDR width does not change when the angular momentum is varied in hot heavy rotating ^{176}W. Reference [14] has also confirmed that the collisional damping does not change with angular momentum and remains equal to the its value at $T=0$. It is, therefore, important to see whether there is some effect, which is not taken into account in the present theories. This is the main motivation for the present work.

The major assumption in the conventional extrapolation of the microscopic framework at zero temperature to nonzero temperature is the replacement of the average over the ground state at $T=0$ by the one over the grand canonical ensemble. This means that the hot GDR has been considered as quantal eigenstates built on top of the thermal equilibrium ensemble. It turned out that if other thermodynamical effects such as thermal fluctuations of shapes, preequilibrium effect, effect of temperature-dependent transferred angular momentum, etc., are not introduced [15–18], the results in these approaches only show weak changes of *quantal* properties of the system at various temperatures. Namely the Landau splitting within the framework of the self-consistent random-phase approximation (RPA) at finite temperature (SC-FTRPA) remains stable with increasing T [19,21]. The spreading width $\Gamma^{\downarrow}$ of the hot GDR, which has been calculated after coupling the ph states to $2p2h$ ones, does not change at finite temperature either [22,23]. It is important to note that in the SC-FTRPA the pp and hh configurations, which appear at finite temperature, have been treated on the same footing as the ph ones. Namely they have been included simultaneously with the ph ones to form the new collective eigenstates generating the hot GDR, although the SC-FTRPA calculations have shown that these pp and hh are mostly *noncollective* [20,24,25]. Thus, it is beyond the capacity of the SC-FTRPA in describing the temperature dependence of the observed GDR width. Exploring the highly excited states in nuclear systems, therefore, one has to examine the *dynamical* effects of temperature by going *beyond* the FTRPA.

Important efforts in this direction have been undertaken in Refs. [26,27]. Vinh Mau [26] has demonstrated that the coupling to the subspace formed by the new configurations leads to the effect of the change of the Fermi sea on the GDR

width. The GDR width has been evaluated in a schematic model at the energy equal to the GDR energy. It has been shown that the Landau damping width of the single GDR mode increases sharply from 0 at $T=0$ up to 4 MeV and saturates at a temperature around $T\sim 6$ MeV. Braghin and Vautherin [27] reexamined the effects due to pp and hh configurations within the SC-FTRPA. Their calculations of the response function of nuclear matter using a schematic Skyrme force have shown that the GDR width is also sensible to the change of the residual interaction. Although there have been several studies on the temperature dependence of the residual forces in hot nuclei (cf. [24,28]), it should be mentioned that so far most of microscopic calculations of the hot GDR characteristics up to $T=5-6$ MeV has been performed using the interaction defined at zero temperature.

The choice of an appropriate decoupling scheme is decisive in the treatment of damping of the hot GDR. One knows that the absence of damping in the mean-field theory and in the standard RPA is an artifact of approximated decoupling schemes due to their incomplete treatment of the residual interaction. If the poles of the Green's function, corresponding to the propagation of collective modes, will be all on the real axis (or slightly below, if one cares about the precise analytical properties of the response function), as in the case of the SC-FTRPA mentioned above, there will not be any damping of the collective modes (cf. also [29]) except for some Landau splitting. The essential step of the present paper is to present a decoupling scheme, which allows one to reveal the mechanism of thermal damping of the hot GDR. The foundation of this scheme is the following. As the temperature increases the quantal effects arising from a tremendous number of noncollective degrees of freedom are expected to diminish, which means they reach the thermal equilibrium much faster than a relatively smaller number of collective degrees of freedom. In the case of the hot GDR, the collective degrees of freedom are the ph phonon states, while the pp and hh configurations consist mostly of noncollective degrees of freedom. The collective degrees of freedom are experimentally relevant, while the noncollective ones are constituting a *background*, to which the collective degrees of freedom are coupled. If the background is very large it can be considered as a *heat bath* and this coupling between collective and noncollective degrees of freedom becomes *irreversible*. This irreversible coupling is responsible for the thermal damping of the hot GDR.

The importance of this concept will become clear in the present paper. Namely, it will be shown that, propagating through the heat bath, the collective RPA ph phonons forming the GDR are strongly polarized by the irreversible coupling to the heat bath via the thermal pp and hh configurations. This phenomenon is characterized by the *polarization* operator, whose presence in the Green's function of the one-phonon propagation leads to a *branch cut* instead of poles along the real axis. Therefore the Green's function has poles only at a finite distance from the real axis. This distance is equal to the imaginary part of the polarization operator and generates the thermal damping, whereas the real part of gives the energy shift. Just because of the thermal effects, the evolution of the collective one-phonon excitation acquires a definite damping (or a lifetime). This feature cannot be obtained, in principle, within the SC-FTRPA, which treats the ph and pp (hh) components on an equal footing.

The formalism is presented in Sec. II, where a microscopic evaluation of thermal damping is developed using the two-time Green's function method [30]. Here, for the sake of generality, the formalism will be derived in the quasiparticle representation including superfluid pairing interaction. We first construct the *thermal ph (phonon) operators*, describing the GDR excitations, within the framework of the standard quasiparticle RPA at finite temperature. We next couple them in an irreversible way to the thermal pp and hh configurations. We obtain a set of equations for two-time Green's functions associated with the evolution of the thermal phonon through the heat bath. From the polarization operator we derive an analytic expression for the damping of the thermal phonon due to the interaction with the heath bath. The physical meaning of the real and imaginary parts of the polarization operator as the energy shift and thermal damping, respectively, is shown in the Appendix, considering an example of damped harmonic oscillator. A semimicroscopic unification of this thermal damping and the usual quantal spreading due to the coupling of ph configurations to $2p2h$ ones is carried out in Sec. III. The formalism is tested by using a simple model with equally degenerate equidistant shells in Sec. IV, where the results of numerical calculations are discussed in comparison with the SC-FTRPA and the experimental systematic. The paper is summarized in the last section.

II. MICROSCOPIC EVALUATION OF THE THERMAL DAMPING WITHIN THE TWO-TIME GREEN'S FUNCTION FORMALISM

We consider the model Hamiltonian consisting of the independent motion of nucleons in the nuclear mean field $H_{\rm MF}$, the superfluid pairing interaction $H_{\rm pair}$, and the residual interaction in the form of the separable multipole force H_M [31]:

$$H=H_{\rm MF}+H_{\rm pair}+H_M\,, \tag{2.1}$$

where

$$H_{\rm MF}=\sum_{jmt_z}[E_j(t_z)-\lambda_{t_z}]a^\dagger_{jm}a_{jm}\,,$$

$$H_{\rm pair}=-\frac{1}{4}\sum_{t_z}G(t_z)\sum_{jmj'm'}a^\dagger_{jm}a^\dagger_{j\tilde{m}}a_{j'\tilde{m}'}a_{j'm'}\,,$$

$$H_M=-\frac{1}{2}\sum_{\lambda\mu}\sum_{t_z\rho=\pm 1}(k_0^{(\lambda)}+\rho k_1^{(\lambda)})M^\dagger_{\lambda\mu}(t_z)M_{\lambda\mu}(\rho t_z)\,. \tag{2.2}$$

In Eqs. (2.1) and (2.2) the standard notation from Ref. [31] is used. Thus, $a^\dagger_{jm}$ and a_{jm} denote the single-particle creation and destruction operators, respectively; t_z is the z projection of the nucleon isospin; $E_j(t_z)$ are single-particle energies; λ_{t_z} are chemical potentials; $G(t_z)$ denote superfluid pairing constants; $k_0^{(\lambda)}$ and $k_1^{(\lambda)}$ stand, respectively, for the isoscalar and isovector constants of the separable multipole forces; $M^\dagger_{\lambda\mu}(t_z)$ are the multipole operators. The tilde denotes the time-reversing operation: $a_{j\tilde{m}}=(-)^{j-m}a_{j-m}$.

In the quasiparticle representation $H_{\rm MF}$ and $H_{\rm pair}$ can be unified to describe the independent quasiparticles motion as

$$H_q = H_{\rm MF} + H_{\rm pair} \simeq \sum_{jm} \epsilon_j \alpha^\dagger_{jm} \alpha_{jm}, \tag{2.3}$$

where $\alpha^\dagger_{jm}$ and α_{jm} are the Bogoliubov quasiparticle operators. The quasiparticle energy ϵ_j is defined by the temperature-dependent BCS (FT-BCS) equations. The multipole operator $M^\dagger_{\lambda\mu}(t_z)$ in Eqs. (2.2) has the form [31]

$$M^\dagger_{\lambda\mu}(t_z) = \frac{(-)^{\lambda-\mu}}{\sqrt{2\lambda+1}} \sum_{jj'}^{t_z} f^{(\lambda)}_{jj'} \Big(\frac{1}{2} u^{(+)}_{jj'} [A^\dagger_{\lambda\mu}(jj') + A_{\lambda\tilde{\mu}}(jj')] + v^{(-)}_{jj'} B^\dagger_{\lambda\mu}(jj') \Big), \tag{2.4}$$

where $f^{(\lambda)}_{jj'} = \langle j' || i R_\lambda(r) || j \rangle$ are the single-particle reduced matrix elements in the separable multipole interaction and $u^{(+)}_{jj'} \equiv u_j v_{j'} + v_j u_{j'}$, $v^{(-)}_{jj'} \equiv u_j u_{j'} - v_j v_{j'}$ with u and v being the Bogoliubov coefficients. The quasiparticle-pair operators are defined as

$$A^\dagger_{\lambda\mu}(jj') = \sum_{mm'} \langle jmj'm' | \lambda\mu \rangle \alpha^\dagger_{jm} \alpha^\dagger_{j'm'},$$

$$B^\dagger_{\lambda\mu}(jj') = \sum_{mm'} \langle jmj'\tilde{m}' | \lambda\mu \rangle \alpha^\dagger_{jm} \alpha_{j'm'}. \tag{2.5}$$

The quasiparticle-scattering operator $B^\dagger_{\lambda\mu}(jj')$ satisfies the following symmetry:

$$B_{\lambda\mu}(jj') = (-)^{j-j'+\lambda} B^\dagger_{\lambda\tilde{\mu}}(j'j). \tag{2.6}$$

In closed-shell nuclei where $u_{j_p} = v_{j_h} = 1$ and $u_{j_h} = v_{j_p} = 0$, the coefficient $u^{(+)}_{jj'}$ corresponds to the ph transition while $v^{(-)}_{jj'}$ is associates with the pp and/or hh ones. Therefore the quasiparticle-pair operators $A^\dagger$ and A are responsible for the ph excitations, whereas the quasiparticle-scattering operators $B^\dagger$ and B correspond to the pp and/or hh ones.

In extending the RPA theory to the nonzero temperature case, the following assumption is adopted for the expectation values of the commutation relations of operators $A^\dagger, A, B^\dagger$, and B, respectively [20,21,24]:

$$\langle [A_{\lambda\mu}(j_a j_b), A^\dagger_{\lambda'\mu'}(j_c j_d)] \rangle = \delta_{\lambda\lambda'} \delta_{\mu\mu'} (1 - n_{j_a} - n_{j_b}) [\delta_{j_a j_c} \delta_{j_b j_d} - (-)^{j_a + j_b - \lambda} \delta_{j_a j_d} \delta_{j_b j_c}], \tag{2.7}$$

$$\langle [B_{\lambda\mu}(j_a j_b), B^\dagger_{\lambda'\mu'}(j_c j_d)] \rangle = \delta_{\lambda\lambda'} \delta_{\mu\mu'} \delta_{j_a j_c} \delta_{j_b j_d} (n_{j_b} - n_{j_a}), \tag{2.8}$$

with n_j being the quasiparticle occupation number at temperature $T = \beta^{-1}$

$$n_j = (e^{\beta\epsilon_j} + 1)^{-1}, \tag{2.9}$$

and $\langle \cdots \rangle$ denoting the thermal average over the grand canonical ensemble:

$$\langle \cdots \rangle = {\rm Tr}[\cdots e^{-\beta H}] / {\rm Tr}[e^{-\beta H}]. \tag{2.10}$$

Let us assume that before undergoing the thermal perturbation produced by the coupling to noncollective pp and hh configurations, the giant resonance, as a superposition of elementary excitations, is generated by the thermal (collective) phonon operator, which has the same ph structure as that of the RPA phonon at zero temperature:

$$Q^\dagger_{\lambda\mu i} = \sum_{jj'} \frac{1}{\sqrt{D_{jj'}}} [x^{\lambda i}_{jj'} A^\dagger_{\lambda\mu}(jj') - y^{\lambda i}_{jj'} A_{\lambda\tilde{\mu}}(jj')]. \tag{2.11}$$

In Eq. (2.11) the renormalization factor

$$D_{jj'} = 1 - n_j - n_{j'} \tag{2.12}$$

is introduced to preserve the boson nature of $Q^\dagger_\nu$ at finite temperature in such a way that the amplitudes x^ν_{ph} and y^ν_{ph} are still satisfying the well-known RPA normalization and closure relations under the expectation value $\langle [A_{ph}, A^\dagger_{p'h'}] \rangle$ in Eq. (2.7).

Applying the standard procedure to derive the RPA equation for the thermal phonon operator with the Hamiltonian in Eq. (2.1), we end up with the FTRPA equation. Its formal structure is the same as the structure of the usual zero-temperature RPA equation, but with a *renormalized* interaction $f^\lambda_{jj'} \sqrt{D_{jj'}}$ instead of $f^\lambda_{jj'}$. The solution of the obtained ph FTRPA equation completely defines the energy ω_ν as well as the amplitudes x^ν_{ph} and y^ν_{ph} of the collective one-phonon excitation generated by the phonon operator $Q^\dagger_\nu$ in Eq. (2.11)

We are now going *beyond* the FTRPA to include the damping emerged from the coupling of the ph FTRPA phonons to the heat bath. Let us express the Hamiltonian in Eq. (2.1) in terms of the thermal phonon operators, which we just defined in the FTRPA above, and quasiparticle-scattering operators. The Hamiltonian (2.1) can be decomposed into three parts, H_R, H_I, and H_{RI}, which describe the motion of the *relevant* (collective) $\{R\}$ and *irrelevant* (noncollective) $\{I\}$ subsystems and their coupling, respectively:

$$H = H_0 + H_{RI}, \quad H_0 \equiv H_R + H_I. \tag{2.13}$$

The explicit form of H_0 and the coupling H_{RI} is

$$H_0 = H_q - \sum_{\lambda\mu ii'} k^{(\lambda)} \mathcal{F}^{(\lambda i)} \mathcal{F}^{(\lambda i')} (Q^\dagger_{\lambda\mu i} + Q_{\lambda\tilde{\mu}i})(Q^\dagger_{\lambda\mu i'} + Q_{\lambda\tilde{\mu}i'}) - \sum_{\lambda\mu} k^{(\lambda)} \sum_{j_1 j_1' j_2 j_2'} \mathcal{G}^{(\lambda)}_{j_1 j_1'} \mathcal{G}^{(\lambda)}_{j_2 j_2'} B^\dagger_{\lambda\mu}(j_1 j_1') B_{\lambda\mu}(j_2 j_2'), \tag{2.14}$$

$$H_{RI} = -\sum_{\lambda\mu i} k^{(\lambda)} \mathcal{F}^{(\lambda i)} \sum_{jj'} \mathcal{G}^{(\lambda)}_{jj'} \times [(Q^\dagger_{\lambda\mu i} + Q_{\lambda\tilde{\mu}i}) B_{\lambda\mu}(jj') + {\rm H.c.}]. \tag{2.15}$$

In Eqs. (2.14) and (2.15) we use the following notations for the vertex functions:

$$\mathcal{F}^{(\lambda i)}=\sum_{jj'}\sqrt{D_{jj'}}F^{(\lambda)}_{jj'}(x^{\lambda i}_{jj'}+y^{\lambda i}_{jj'}), \tag{2.16}$$

$$F^{(\lambda)}_{jj'}=\frac{1}{2\sqrt{2}\sqrt{2\lambda+1}}f^{(\lambda)}_{jj'}u^{(+)}_{jj'},$$

$$\mathcal{G}^{(\lambda)}_{jj'}=\frac{1}{\sqrt{2}\sqrt{2\lambda+1}}f^{(\lambda)}_{jj'}v^{(-)}_{jj'}. \tag{2.17}$$

The vertex $\mathcal{G}^{(\lambda)}_{jj'}$ has a symmetry property

$$\mathcal{G}^{(\lambda)}_{jj'}=(-)^{j-j'+\lambda}\mathcal{G}^{\lambda}_{j'j}. \tag{2.18}$$

The thermal damping of the phonon excitation can be studied introducing the following two-time Green's functions, which associate with *(1) the propagation of a free phonon through the hot nuclear media,*

$$G^{-}_{\lambda i;\lambda' i'}(t,t')=\langle\langle Q_{\lambda\mu i}(t);Q^{\dagger}_{\lambda'\mu' i'}(t')\rangle\rangle, \tag{2.19}$$

(2) the coupling of a phonon with the quasiparticle-scattering process,

$$\Gamma^{-}_{jj'\lambda;\lambda' i'}(t,t')=\langle\langle B_{\lambda\mu}(jj')(t);Q^{\dagger}_{\lambda'\mu' i'}(t')\rangle\rangle, \tag{2.20}$$

and with their backward processes, namely: *(3) the backward free-phonon propagation,*

$$G^{+}_{\lambda i;\lambda' i'}(t,t')=\langle\langle Q^{\dagger}_{\lambda\tilde{\mu} i}(t);Q^{\dagger}_{\lambda'\mu' i'}(t')\rangle\rangle, \tag{2.21}$$

(4) the backward quasiparticle-phonon transition:

$$\Gamma^{+}_{jj'\lambda;\lambda' i'}(t,t')=\langle\langle B^{\dagger}_{\lambda\tilde{\mu}}(jj')(t);Q^{\dagger}_{\lambda'\mu' i'}(t')\rangle\rangle. \tag{2.22}$$

Since we have regarded the ph phonons as quasibosons in the FTRPA, in the following we will consider $[Q_{\lambda\mu i},B_{\lambda'\mu' i'}(jj')]=0$. Applying the standard method to derive the equations for two-time Green's functions $\langle\langle\mathcal{A}(t);\mathcal{B}(t')\rangle\rangle$ with the Hamiltonian in Eqs. (2.14) and (2.15), we derive an hierarchy of Green's functions, which contains not only the functions (2.19)–(2.22) but also the higher-order ones, such as $\langle\langle BQ;Q^{\dagger}\rangle\rangle$, $\langle\langle QQ;Q^{\dagger}\rangle\rangle$, $\langle\langle BQQ;Q^{\dagger}\rangle\rangle$, etc. In order to close this hierarchy we use Eq. (2.8) to decouple, e.g.,

$$\langle\langle[B_{\lambda\mu}(j_aj_b),B_{\lambda'\mu'}(j_cj_d)]Q_{\lambda\mu i};Q^{\dagger}_{\lambda\mu i}\rangle\rangle = \delta_{j_aj_c}\delta_{j_bj_d}(n_{j_b}-n_{j_a})\langle\langle Q_{\lambda\mu i};Q^{\dagger}_{\lambda\mu i}\rangle\rangle. \tag{2.23}$$

In this way we obtain a closed set of equations for the two-time Green's functions in Eqs. (2.19)–(2.22). Making the Fourier transformation to the energy variable η, we end up with a complete set of four equations for the Fourier components of the Green's functions. They are

$$(\eta-\omega_{\lambda i})G^{-}_{\lambda i;\lambda i}(\eta)+2k^{(\lambda)}\mathcal{F}^{(\lambda i)}\sum_{jj'}\mathcal{G}^{(\lambda)}_{jj'}\Gamma^{-}_{jj'\lambda;\lambda i}(\eta)=\frac{1}{2\pi}, \tag{2.24}$$

$$(\eta-\epsilon_j+\epsilon_{j'})\Gamma^{-}_{jj'\lambda;\lambda i}(\eta)-2(n_j-n_{j'})k^{(\lambda)}\mathcal{G}^{(\lambda)}_{jj'} \times\left(\sum_{i'}\mathcal{F}^{(\lambda i')}[G^{-}_{\lambda i';\lambda i}(\eta)+G^{+}_{\lambda i';\lambda i}(\eta)]+\frac{1}{2}\sum_{j_1j_1'}\mathcal{G}^{(\lambda)}_{j_1j_1'}[\Gamma^{-}_{j_1j_1'\lambda;\lambda i}(\eta)+\Gamma^{+}_{j_1j_1'\lambda;\lambda i}(\eta)]\right)=0, \tag{2.25}$$

$$(\eta+\omega_{\lambda i})G^{+}_{\lambda i;\lambda i}(\eta)-2k^{(\lambda)}\mathcal{F}^{(\lambda i)}\sum_{jj'}\mathcal{G}^{(\lambda)}_{jj'}\Gamma^{+}_{jj'\lambda;\lambda i}(\eta)=0, \tag{2.26}$$

$$(\eta+\epsilon_j-\epsilon_{j'})\Gamma^{+}_{jj'\lambda;\lambda i}(\eta)+2(n_j-n_{j'})k^{(\lambda)}\mathcal{G}^{(\lambda)}_{jj'}\left(\sum_{i'}\mathcal{F}^{(\lambda i')}[G^{-}_{\lambda i';\lambda i}(\eta)+G^{+}_{\lambda i';\lambda i}(\eta)]+\frac{1}{2}\sum_{j_1j_1'}\mathcal{G}^{(\lambda)}_{j_1j_1'}[\Gamma^{-}_{j_1j_1'\lambda;\lambda i}(\eta)+\Gamma^{+}_{j_1j_1'\lambda;\lambda i}(\eta)]\right) =0. \tag{2.27}$$

Using Eqs. (2.6) and (2.18), and $\Gamma^{+}_{jj'\lambda;\lambda i}(\eta)=(-)^{j-j'+\lambda}\Gamma^{-}_{j'j\lambda;\lambda i}(\eta)$, it is easy to see that Eq. (2.27) is just Eq. (2.25) with interchanged indices $j\leftrightarrow j'$. Therefore, one can also express $G^{+}_{\lambda i;\lambda i}(\eta)$ in Eq. (2.26) in terms of $\Gamma^{-}_{jj'\lambda;\lambda i}(\eta)$ as

$$G^{+}_{\lambda i;\lambda i}(\eta)=\frac{2k^{(\lambda)}\mathcal{F}^{(\lambda i)}}{\eta+\omega_{\lambda i}}\sum_{jj'}\mathcal{G}^{(\lambda)}_{jj'}\Gamma^{-}_{jj'\lambda;\lambda i}(\eta). \tag{2.28}$$

Substituting Eq. (2.28) for Eq. (2.24), we get the final set of two equations for the Green's functions $G^{-}_{\lambda i;\lambda i}(\eta)$ and $\Gamma^{-}_{jj'\lambda;\lambda i}(\eta)$ in the form

$$(\eta-\omega_{\lambda i})G^{-}_{\lambda i;\lambda i}(\eta)+2k^{(\lambda)}\mathcal{F}^{(\lambda i)}\sum_{jj'}\mathcal{G}^{(\lambda)}_{jj'}\Gamma^{-}_{jj'\lambda;\lambda i}(\eta)=\frac{1}{2\pi}, \tag{2.29}$$

$$(\eta-\epsilon_j+\epsilon_{j'})\Gamma^{-}_{jj';\lambda i}(\eta)-2(n_j-n_{j'})k^{(\lambda)}\mathcal{G}^{(\lambda)}_{jj'}\left([1+\zeta_{\lambda i}(\eta,\omega_{\lambda i})]\sum_{j_1j_1'}\mathcal{G}^{(\lambda)}_{j_1j_1'}\Gamma^{-}_{j_1j_1';\lambda i}(\eta)+\sum_{i'}\mathcal{F}^{(\lambda i')}G^{-}_{\lambda i';\lambda i}(\eta)\right)=0. \tag{2.30}$$

The factor $\zeta_{\lambda i}(\eta,\omega_{\lambda i})$ in Eq. (2.30) arises from the backward process of phonon propagation in Eq. (2.21). It has the form

$$\zeta_{\lambda i}(\eta,\omega_{\lambda i})=\frac{2k^{(\lambda)}}{\eta+\omega_{\lambda i}}\mathcal{F}^{(\lambda i)}\sum_{i'}\mathcal{F}^{(\lambda i')}. \tag{2.31}$$

The RHS of Eq. (2.31) shows that, for positive energies η and $\omega_{\lambda i}$, the contribution of this factor is proportional to $O[(x^{(\lambda i)}_{jj'}+y^{(\lambda i)}_{jj'})^2]$, which is a second-order effect in terms of the phonon amplitudes $x^{(\lambda i)}_{jj'}$ and $y^{(\lambda i)}_{jj'}$.

The set of equations (2.29) and (2.30) represents the basic equations for Green's functions in our formalism, which allow one to study the damping of the thermal phonon excitations beyond the FTRPA. This can be seen clearly by considering the propagation of a phonon with number $i'=i$ and multipolarity λ. Eliminating the function $\Gamma^{-}_{j_1j_1';\lambda i}(\eta)$ from Eqs. (2.29) and (2.30) by expressing it in terms of $G^{-}_{\lambda i';\lambda i'}(\eta)$, we obtain the equation

$$[\eta-\omega_{\lambda i}-P_{\lambda i}(\eta)]G^{-}_{\lambda i;\lambda i}(\eta)=\frac{1}{2\pi}. \tag{2.32}$$

The polarization operator $P_{\lambda i}(\eta)$ in Eq. (2.32) has the explicit form as

$$P_{\lambda i}(\eta)=-4[k^{(\lambda)}\mathcal{F}^{(\lambda i)}]^2\frac{\Sigma_{jj'}[\mathcal{G}^{(\lambda)}_{jj'}]^2(n_j-n_{j'})/(\eta-\epsilon_j+\epsilon_{j'})}{1-2[1+\zeta_{\lambda i}(\eta,\omega_{\lambda i})]k^{(\lambda)}\Sigma_{jj'}[\mathcal{G}^{(\lambda)}_{jj'}]^2(n_j-n_{j'})/(\eta-\epsilon_j+\epsilon_{j'})}. \tag{2.33}$$

The quantity η denotes the polarized thermal phonon energy under the thermal effects due to the coupling H_{RI} in Eq. (2.15). It is defined from the secular equation:

$$\eta-\omega_{\lambda i}-P_{\lambda i}(\eta)=0. \tag{2.34}$$

The explicit expression for the *thermal damping* $\gamma_{\lambda i}$ of the thermal one-phonon excitation is the imaginary part of the analytical continuation of the polarization $P_{\lambda i}(\eta)$ into the complex energy plane

$$P_{\lambda i}(\eta\pm i\varepsilon)=P_{\lambda i}(\eta)\mp i\gamma_{\lambda i}(\eta). \tag{2.35}$$

Using the symbolical identity

$$\frac{1}{\eta-\omega\pm i\varepsilon}=\mathcal{P}\frac{1}{\eta-\omega}\mp i\pi\delta(\eta-\omega), \tag{2.36}$$

with $\varepsilon\to 0$, we get the expression for the damping $\gamma_{\lambda i}(\eta)$ in the form

$$\gamma_{\lambda i}(\eta)=-4\pi\frac{k^{(\lambda)}[\mathcal{F}^{(\lambda i)}]^2R^{(\lambda)}(\eta)}{\{1-2[1+\zeta_{\lambda i}(\eta,\omega_{\lambda i})]L^{(\lambda)}(\eta)\}^2+4\pi^2\{[1+\zeta_{\lambda i}(\eta,\omega_{\lambda i})]R^{(\lambda)}(\eta)\}^2}, \tag{2.37}$$

where

$$R^{(\lambda)}(\eta)=k^{(\lambda)}\sum_{jj'}[\mathcal{G}^{(\lambda)}_{jj'}]^2(n_j-n_{j'})\,\delta(\eta-\epsilon_j+\epsilon_{j'}), \tag{2.38}$$

$$L^{(\lambda)}(\eta)=k^{(\lambda)}\sum_{jj'}[\mathcal{G}^{(\lambda)}_{jj'}]^2(n_j-n_{j'})\mathcal{P}\frac{1}{\eta-\epsilon_j+\epsilon_{j'}}, \tag{2.39}$$

and $\mathcal{P}$ indicates the principal value of the corresponding integral. The poles of the polarization operator $P_{\lambda i}(\eta)$ in Eq. (2.33) correspond to the pp and hh levels at finite temperature when the H_{RI} is switched off. The damping $\gamma_{\lambda i}$ of the thermal one-phonon excitation vanishes in cold nuclei as the factor $(n_j-n_{j'})$ in Eqs. (2.33) and (2.37) becomes zero at $T=0$. In the Appendix, we show, by considering the simple example of a damped harmonic oscillator, that the imaginary part of the analytical continuation of the polarization operator into the complex energy plane is indeed the thermal damping, while its real part gives the energy shift.

The strength function, corresponding to the damping of thermal phonon, has the Lorenzian form as

$$S_{\lambda i}(\eta)=\frac{1}{\pi}\frac{\gamma_{\lambda i}(\eta)}{[\eta-\omega_{\lambda i}-P_{\lambda i}(\eta)]^2+\gamma^2_{\lambda i}(\eta)}, \tag{2.40}$$

which provides the information about the evolution of the hot GDR.

The thermal damping width $\Gamma_{\lambda}^{\mathrm{ITD}}$ integrated over the energy interval (E_1,E_2), where the GDR is localized is now calculated using the strength function in Eq. (2.40) as

$$\Gamma_{\lambda i}^{\mathrm{ITD}}=\sqrt{\frac{m_k(\lambda i)}{m_0(\lambda i)}-\overline{E^2}}, \tag{2.41}$$

where

$$m_k(\lambda i)=\int_{E_1}^{E_2} S_{\lambda i}(\eta)\,\eta^k d\eta \tag{2.42}$$

is the k moment, and

$$\overline{E}=\frac{m_1(\lambda i)}{m_0(\lambda i)} \tag{2.43}$$

is the energy centroid. Hereafter we call the width $\Gamma_{\mu}^{\mathrm{ITD}}$ the *integrated thermal damping width.*

The results obtained above are different from solving the conventional SC-FTRPA equation in two steps. The reason is the SC-FTRPA considers the pp and hh configurations at finite temperature as elementary excitations on the same footing with the ph ones. Therefore the pp and hh configurations in the SC-FTRPA partly participate to the collective motion restoring the strength and collectivity. The normalization condition within the conventional SC-FTRPA contain, beside the amplitudes $x_{jj'}^{\lambda i}$ and $y_{jj'}^{\lambda i}$, also the amplitude $\psi_{jj'}^{\lambda i}$ and $\phi_{jj'}^{\lambda i}$, arising from the operators $B_{jj'}^{+}(\lambda i)$ and $B_{jj'}(\lambda i)$, respectively. Therefore no thermal damping width for the SC-FTRPA modes can take place [19–25]. In our formalism, the pp and hh configurations are expressed in terms of noncollective degrees of freedom. Consequently, they do not participate in constructing the collective ph excitations. Therefore they are treated *beyond* the ph FTRPA. Under this treatment they induce an irreversible coupling H_{RI} of collective ph phonon to the noncollective subspace, constituting the heat bath. This phonon-heat bath coupling leads to the thermal damping of the ph phonon in the collective subspace after projecting out the noncollective degrees of freedom [function $\Gamma_{ss';\nu'}^{-}(\eta)$]. This situation is very similar to the quantal spreading (at $T=0$), which occurs in the $1p1h$ subspace, when the ph RPA phonons are coupled to the $2p2h$ (two-phonon) configurations beyond RPA. The latter is however reversible because of the limitation of the $2p2h$ space.

As the apparent width of the GDR observed in highly excited nuclei contains both the quantal spreading width $\Gamma^{\downarrow}$ and the integrated thermal damping width $\Gamma_{\mu}^{\mathrm{ITD}}$, it is useful to unify these two mechanisms in one single description of the total width. This is done in the next section.

III. SEMIMICROSCOPIC UNIFICATION OF QUANTAL AND THERMAL DAMPINGS

A consistent microscopic unification of quantal and thermal dampings requires a systematic derivation of the total width, which contains both quantal spreading and thermal damping widths in a microscopic way. In the present work we restrict ourselves only by combining the quantal spreading width Γ_Q existing at zero temperature with the thermal damping width $\Gamma_{\mu}^{\mathrm{ITD}}$ of the GDR at nonzero temperature, discussed in the previous section. For the quantal spreading width Γ_Q, we assume it is given separately within the framework of some microscopic approach such as in Refs. [23]. The standard theory [32] for evaluating strength functions is applied for folding two quantal and thermal distributions of the GDR in hot nuclei as follows.

According to the compound nucleus hypothesis, we may assume that the compound nuclear state $|c(E^*)\rangle$ at the excitation energy E^* is given as a combination of excited multiquasiparticle states $|\mu(E^*)\rangle$

$$|c(E^*)\rangle=\sum_{\mu} X_{\mu}^{c}|\mu(E^*)\rangle. \tag{3.1}$$

The dipole-dipole residual interaction beyond the thermal mean field leads to the $B(E1)$ distribution for each multiquasiparticle state $|\mu(E^*)\rangle$ over the higher-lying ones. If the multiquasiparticle states are associated with the collective thermal phonon ones as within the framework of FTRPA (i.e., $\langle\mu'|\cdots|\mu\rangle=\langle Q_{\mu'}\cdots Q_{\mu}^{\dagger}\rangle$), this corresponds to the distribution of thermal one-phonon excitations

$$|c\rangle=\sum_{\mu} X_{\mu}^{c}|\mu\rangle, \tag{3.2}$$

where in the case of rotation the state $|\mu\rangle$ in general has three spherical components, i.e., $|\mu\rangle\equiv|\mu,k\rangle$ with $k=1$, 2, and 3. This distribution would represent the GDR built on top of the compound levels in Eq. (3.1) if the description of the GDR as stationary quantal eigenstates (i.e., without thermal damping) were valid. In that case the GDR would couple only to particular quantal doorway states, containing the low-lying surface vibrations. The GDR acquires then a *quantal* (spreading) width Γ_Q. In reality, this will not be a general situation because the nuclear shape fluctuations [34], rotational damping [33,35] as well as the irreversible coupling to pp and hh configurations, proposed in the present work may cause the variation of the GDR frequencies within the ensemble of compound states. The result is an *additional spreading* width of the GDR over compound states under the effects of shape fluctuations and/or rotational damping or the *thermal damping* (a definite lifetime) of the GDR caused by the irreversible coupling H_{RI} in Eq. (2.15).

Based on this point of view we apply the system of equations for evaluating the strength functions of the GDR within the *motional damping* scheme, given by the standard theory [32] following Refs. [34,35] as

$$P(E)=\frac{1}{2\pi}\,\frac{\Gamma}{(E-\overline{E}-\delta E)^2+(\frac{1}{2}\Gamma)^2}, \tag{3.3}$$

$$\Gamma=\Gamma_Q+[\Delta\omega_0]^2\int_{-\infty}^{+\infty}P(x+\overline{E})\,\frac{2\Gamma_{\mu}}{(E-x)^2+\Gamma_{\mu}^2}\,dx, \tag{3.4}$$

$$\delta E=[\Delta\omega_0]^2\int_{-\infty}^{+\infty}P(x+\overline{E})\,\frac{E-x}{(E-x)^2+\Gamma_{\mu}^2}\,dx. \tag{3.5}$$

Here as in Refs. [34,35] $P(E)$ is the strength distribution of the GDR, localized at the energy $E=\overline{E}$. The quantity $\Delta\omega_0$ denotes the average deviation of the phonon energy $\Delta\omega_0=\sqrt{\langle(\eta-\omega)^2\rangle}$. Since we are only focusing on the effects of the coupling H_{RI}, the thermal damping of the GDR states $|\mu\rangle$ over the compound nucleus state $|c\rangle$ is characterized by the integrated thermal damping width $\Gamma_\mu=\Gamma_\mu^{\rm ITD}$ alone, which has been calculated microscopically in the previous section. Finally, the quantity Γ_Q is the quantal spreading width associated with the coupling to more complicated states such as $(2p2h)$ ones (cf. also Ref. [36]).

It should be mentioned that at high temperature (above around $T=5$ MeV) the disappearance of shell effects turns the energy functional into the one given by the liquid drop model. In the theory of Fermi liquids the damping of giant resonances is described as the absorption of the nuclear zero sound. The absorption coefficient γ for a single GDR mode with energy η is found analytically from the Landau collisional integral as

$$\gamma=a[\,\eta^2+(2\pi T)^2], \tag{3.6}$$

where the first term $a\eta^2$ corresponds to the damping of the GDR in the cold system whereas the second term contains a T^2 dependence of the damping at finite temperature. We note, however, that the effects due to the finiteness of the nucleus were ignored in Eq. (3.6). These effects are known to be responsible for large thermal fluctuations, which contribute significantly in enlarging the width of the hot GDR. Unfortunately, to our best knowledge, a fully microscopic derivation of the parameter γ in hot nuclei is still absent and, in general, more detailed investigations are called for. In finite surface dominated systems, for instance, a linear dependence on η and T for γ in Eq. (3.6) has been suggested in Ref. [22]. However the numerical calculations in realistic hot nuclei [23] have shown that the fragmentation of the hot GDR does not change much with varying temperature up to around 3 MeV even with the T^2 dependence of γ as in Eq. (3.6) taken into account. Therefore it is unlikely that there will be a significant change in the width of the hot GDR at $T\sim 4-5$ MeV after including the T^2 dependence except that the fine structure of the GDR distribution is smeared out [28]. Taking into account these results and also the fact that in the present paper we concentrate the attention only on the thermal damping mechanism due to the coupling of collective ph modes to the noncollective pp and hh configurations, we do not include the T^2 dependence here.

The exact solution of the system described by Eqs. (3.3)–(3.5) has been studied in Ref. [35]. In order to find a good starting point for the iteration procedure, it has been suggested to substitute Eq. (3.3) for Eqs. (3.4) and (3.5). When the main contribution to the integrals in Eqs. (3.4) and (3.5) comes around $x\approx E$ after this substitution, one may set the energy shift $\delta E(x)\approx\delta E(E)$ and $\Gamma(x)\approx\Gamma(E)$ in the integrand. In this case both integrals can be carried out analytically. The result is the linear equations for the initial values of Γ and δE, which already provide a good approximation to the exact solution so that only few iterations are needed. With the present form of Eqs. (3.3)–(3.5), we obtain for the initial values of Γ and δE simpler expressions than those given in Ref. [35]. They are

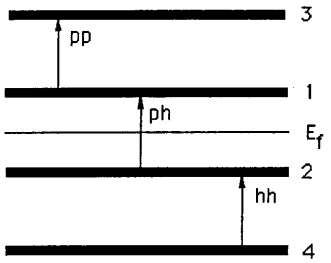

FIG. 1. Schematic model under consideration.

$$\Gamma=\Gamma_Q+[\Delta\omega_0]^2\frac{\Gamma+2\Gamma_\mu^{\rm ITD}}{[(E-\overline{E}-\delta E)^2+(\frac{1}{2}\Gamma+\Gamma_\mu^{\rm ITD})^2]}, \tag{3.7}$$

$$\delta E=\frac{(\Gamma-\Gamma_Q)(E-\overline{E})}{2(\Gamma+\Gamma_\mu^{\rm ITD})-\Gamma_Q}. \tag{3.8}$$

Before evaluating Eqs. (3.7) and (3.8) in the next section, it is worth mentioning how the damping width Γ_μ in Eqs. (3.4) and (3.5) has been evaluated so far. In Ref. [34] the thermal fluctuations of the nuclear shape have been considered for a hot nucleus with mass $A=110$ carrying no angular momentum. The estimation $\Gamma_\mu\simeq 1.7T^3$ and $\Delta\omega_0\simeq 1.3\sqrt{T}$ extracted from the Fermi gas model has been used. The FWHM of the GDR obtained by solving Eqs. (3.4) and (3.5) with these value of Γ_μ and $\Delta\omega_0$ has shown an effect due to motional *narrowing*. Namely, the FWHM at $T\geqslant 2$ MeV is almost equal to its value at $T=0$. Meanwhile the calculations with $\Gamma_\mu=0$ in Eqs. (3.4) and (3.5) gave a FWHM of GDR, which grows almost linearly with increasing temperature. Both of these results disagree with the temperature dependence of the apparent width of the GDR, which has been observed in experiments [2–8].

IV. NUMERICAL CALCULATIONS FOR THE GDR WIDTH IN HOT NUCLEI WITHIN A SCHEMATIC MODEL

In this section we apply the proposed approach to a simplest realization for the hot GDR in a system with mass $A=112$, which is provided by the schematic model in Fig. 1. It consists of four Ω-generate equidistant shells, which are symmetrically located at both sides of the Fermi level and interact via the separable dipole-dipole force with the same matrix element in the dipole operator in Eq. (2.4): $f_{12}=f_{13}=f_{24}=f$. Here the subscripts 1 and 3 numerate the two shells above the Fermi level, while 2 and 4 those below it. This model generates one collective ph phonon excitation (the transition $2\rightarrow 1$), which is coupled to the thermal pp (the transition $1\rightarrow 3$) and hh (the transition $4\rightarrow 2$) configurations. The energies of four shells are, respectively, $\epsilon_1=-\epsilon_2=E/2$, $\epsilon_3=-\epsilon_4=3E/2$ with a value $E=6$ MeV, chosen as the distant between shell. The FTRPA equation and Eq. (2.34) have analytical solutions in this model.

The parameter $C=\frac{2}{3}k(\Omega f)^2$ of the dipole interaction is adjusted in such a way that the phonon energy

$$\omega=E\sqrt{1-C\frac{(1-2n_1)}{E}},\quad n_1=(e^{\beta\epsilon_1}+1)^{-1} \tag{4.1}$$

reproduces the empirical energy $\overline{E}_{\rm GDR}$ of the GDR at $T=0$: $\omega_{T=0}=\overline{E}_{\rm GDR}=$ 16 MeV. This value of $C_{T=0}$ is extrapolated to $T\neq 0$.

The thermal damping in Eq. (2.37) is given by

$$\gamma(\eta)=\frac{\varepsilon C^2E^2\eta(1-2n_1)(n_1-n_3)r(\eta,E,\varepsilon)}{2\omega\{[1+2CEz(\eta,\omega)/(\eta^2-E^2)]^2r^2(\eta,E,\varepsilon)+[4\varepsilon CE\eta z(\eta,\omega)]^2\}}, \tag{4.2}$$

where

$$r(\eta,E,\varepsilon)=[(\eta+E)^2+\varepsilon^2][(\eta-E)^2+\varepsilon^2], \tag{4.3}$$

$$z(\eta,\omega)=[1+\zeta(\eta,\omega)](n_1-n_3), \tag{4.4}$$

and the representation

$$\delta(\eta)=\frac{1}{2\pi i}\left(\frac{1}{\eta-i\varepsilon}-\frac{1}{\eta+i\varepsilon}\right)=\frac{1}{\pi}\frac{\varepsilon}{\eta^2+\varepsilon^2} \tag{4.5}$$

is applied for the δ function.

The factor ζ in Eq. (2.31) arising from the backward process in Eq. (2.21) is

$$\zeta(\eta,\omega)=\frac{CE(1-2n_1)}{8\omega(\eta+\omega)}, \tag{4.6}$$

and the polarization operator in Eq. (2.33) has the form

$$P(\eta)=\frac{(\eta+\omega)C^2E^2(1-2n_1)(n_1-n_3)}{4\omega(\eta+\omega)[\eta^2-E^2+2CE(n_1-n_3)]+C^2E^2(1-2n_1)(n_1-n_3)}. \tag{4.7}$$

The finite ε in Eqs. (4.2), (4.3), and (4.5) plays a role of a smearing parameter in calculating the strength function. It can also account for coupling of $2p2h$ states to even more complicated configurations. In numerical calculations in realistic nuclei, to avoid spurious results, ε is usually chosen to be sufficiently small ($0.1\leqslant\varepsilon\leqslant 1$ MeV) such as the lowest moments of the strength function are insensitive to its actual value. In the following we choose $\varepsilon=1$ MeV and the shell distance $E=6$ MeV. The GDR centroid energy at $T=0$ has been taken from the (γ,n) reaction data for Sn isotopes [37] as $\overline{E}_{\rm GDR}=16$ MeV.

The solutions of Eq. (2.34) are presented in Fig. 2 as a function of temperature. The level with energy equal to 16 MeV at $T=0$ corresponds to the GDR energy, while the one with energy $E=6$ MeV at $T\rightarrow 0$ arises from the pp and hh configurations. As seen from Fig. 2, the temperature dependence of the GDR energy becomes weaker by switching-on the coupling to the thermal quasiparticle-scattering field (compare thick and thin curves). The dashed curves are obtained without the factor ζ in the polarization operator. The comparison between solid and dashed curves shows that the effect due to the backward process in Eq. (2.21) on the energy levels is negligible.

The strength function within the conventional SC-FTRPA at several temperatures and the $m_0(1^-)$-moment as a function of T are depicted in Fig. 3. Since the $m_0(1^-)$-moment decreases slightly at $T\geqslant 2$ MeV, the total strength of the distribution $\mathcal{S}(1^-,\omega)$ also decreases as T increases. In order to keep the EWSR temperature independent, we renormalize the strength function $\mathcal{S}(1^-,\omega)$, dividing it by $m_0(1^-)$. The result is shown at the bottom of Fig. 3. As expected, apart from a downward shift of the GDR localization, no change in the GDR shape occurs in the SC-FTRPA. The shift of the GDR energy takes place since we have fixed the parameter $C=C_{T=0}$. One could readjust the parameter C so as to reproduce the GDR energy at each temperature within the FTRPA. This would increase the absolute value of C ($C<0$), indicating an increase of the dipole-dipole correlations at finite temperature. As the study of the temperature dependence of the effective forces is not complete, we prefer to keep the parameter C independent of temperature.

We calculated the damping $\gamma(\eta)$ from Eq. (4.2) and the polarization operator $P(\eta)$ from Eq. (4.7) as a function of temperature. The obtained values are used to calculate the strength function in Eq. (2.40), which describes the damping of the thermal one-phonon excitation. The results of the calculation of the strength function at several temperatures are displayed in Fig. 4. The high-lying peak of this strength function corresponds to the GDR. It has no width at $T\rightarrow 0$ and becomes broader noticeably with increasing the temperature. At the same time there appears a new peak caused by the pp and hh transitions in the low energy region at around

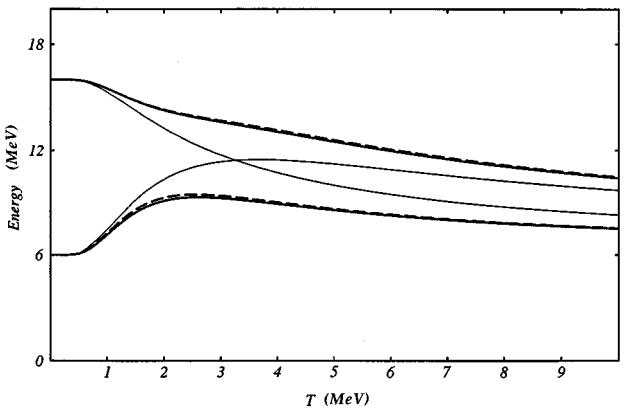

FIG. 2. Energy levels as a function of temperature. Thin curves correspond to the case when the interaction is switched off. The energies η from Eq. (2.34) with and without backward process are given by the thick solid and dashed curves, respectively.

8 MeV, which arises from the level with energy equal to 6 MeV at $T\rightarrow 0$ and can be regarded as the oversimplified influence of the noncollective degrees of freedom in hot nuclei. A clear transfer of the strength from the region of GDR to the low-lying peak is observed at $T>2$ MeV. The strength of the GDR peak is reduced while the strength concentrated on the low-lying mode increases with increasing tempera-

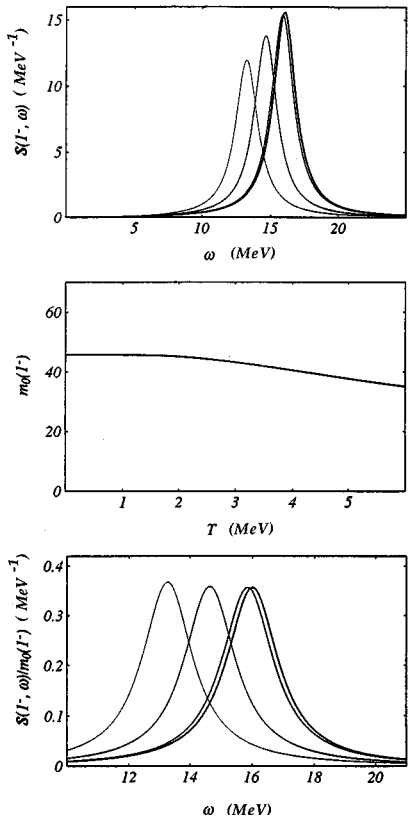

FIG. 3. SC-FTRPA strength function (top) at several temperatures $T=0$, 2, 4, and 6 MeV and the moment $m_0(1^-)$ as a function of temperature (middle). The renormalized strength function $\mathcal{S}(1^-,\omega)\times m_0(1^-)$ is depicted at the bottom. In the top and bottom parts, a thinner curve represents the result obtained at a higher temperature.

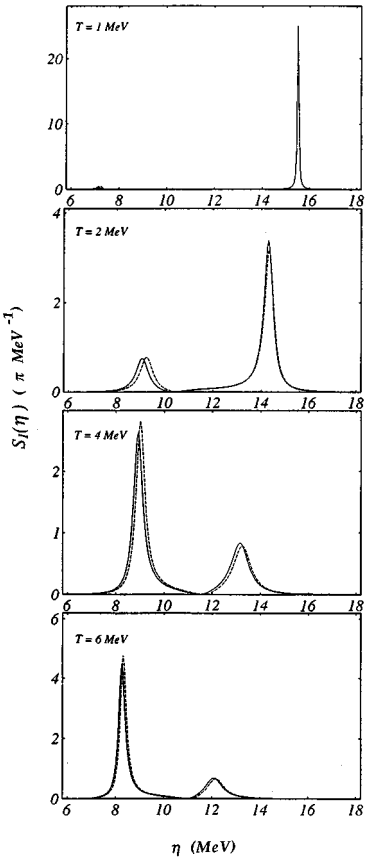

FIG. 4. Strength function $S_1(\eta)$ in Eq. (2.40) at several temperatures T.

ture, preserving the total integrated strength in the whole energy region from 0 up to 20 MeV. At $T\geqslant 4-6$ MeV the peak corresponding to the GDR is disappearing as its strength is almost exhausted by the low-lying mode. The appearance of this low-lying mode in our schematic model is interesting in the sense that it leads to a loss of strength of the GDR peak in hot nuclei and ultimately to its disappearance at high temperature. As this mode is located below 10 MeV its deexcitation must be within the low energy component of the γ spectra, which is mainly coming from the statistical decay of the final nuclei formed after particle decay from the compound system. Since in realistic nuclei there are many pp and hh configurations at finite temperature, the low-lying states are not concentrated in one single mode, but strongly fragmented. This makes the observation of these low-lying modes difficult. In fact, after subtracting the low-energy component and the high-lying one due to the proton-neutron bremsstrahlung [6–8], the GDR in the energy interval $10\leqslant E_\gamma\leqslant 20$ MeV has been observed and its collectivity is reduced at high excitation energy [38]. A possibility for the low-lying component around 8 MeV in the γ spectrum at high temperature, which absorbs the main strength of the GDR, has been the subject of recent discussions by the MEDEA Collaboration at the GANIL facility [8].

In order to see the detail behavior of the thermal damping of the GDR we calculated the integrated thermal damping width $\Gamma_\mu^{\rm ITD}$ in Eq. (2.41) using the obtained strength function. The results are displayed in Fig. 5. It is important to properly define the energy region of the GDR in performing the inte-

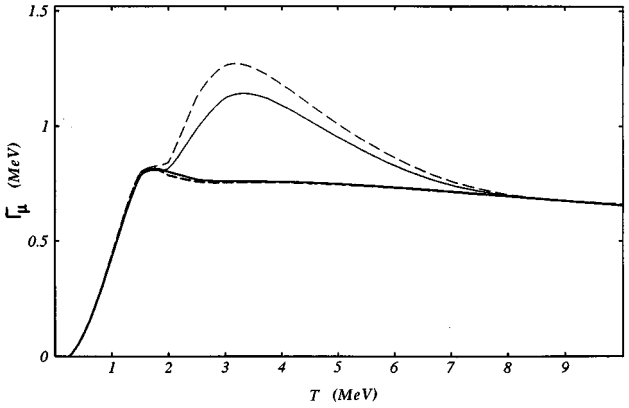

FIG. 5. Integrated thermal damping width $\Gamma_\mu^{\rm ITD}$ as a function of temperature. Solid curves are obtained with the factor ζ, while the dashed curves are without this factor. Thick curves (solid and dashed) represent the results, where the lower integration limit in Eq. (2.42) is chosen as the pole of the polarization operator in Eq. (4.7). Thin curves (solid and dashed) are obtained after carrying out the integration within the fixed interval $10 \leqslant \omega \leqslant 20$ MeV.

gration. Irrespectively of the value of the thermal damping $\gamma(\eta)$, a separation of the GDR and the low-lying peak (see Fig. 4) is always possible by the poles of the polarization operator in Eq. (4.7), at which the strength function in Eq. (2.40) becomes zero. The temperature dependence of this pole is illustrated in Fig. 2 by the thin curve, started from 6 MeV. This energy provides us with the proper lower limit of the integration in Eq. (2.42) while the upper limit is fixed at 20 MeV. As seen in Fig. 5, the integrated thermal damping width of the GDR (thick curves) increases strongly with increasing temperature up to around $T \sim 2$ MeV. At $T \sim 2-2.5$ MeV the GDR integrated thermal damping width $\Gamma_\mu^{\rm ITD}$ clearly reaches a saturated value. In the high-temperature region $T \geqslant 6$ MeV, where the GDR is disappearing (Fig. 4), it starts to decrease very slowly. It would not be accurate to carry out the integration over the fixed energy interval $10 \leqslant E_\gamma \leqslant 20$ MeV since there is an additional contribution from the tail of the low-lying mode (see Fig. 4). This contribution would lead to an enhancement of the width at around $T \sim 3-4$ MeV (thin curve in Fig. 5). The contribution from the low-lying mode should be eliminated in the discussion of the GDR width. The strength function and the integrated thermal damping width practically do not change by neglecting the effects due to the backward phonon propagation ($\zeta = 0$) (dashed curves in Figs. 3 and 5).

The numerical calculations clearly show that the coupling H_{RI} [Eq. (2.15)] of the hot GDR to noncollective degrees of freedom in the heat bath leads to a manifestation of the temperature dependence for the GDR damping. Moreover this thermal damping reproduces quite well the tendency observed in the experiments. Namely, the thermal damping width of the GDR increases sharply with increasing temperature T up to around 2–2.5 MeV and reaches a saturation at higher temperatures. For a comparison, it is worth mentioning that the temperature at which the thermal damping width of the GDR reaches the saturation as well as the saturated value for the damping width itself are considerably *lower* than those calculated in Ref. [26]. The saturation of the GDR thermal damping width has a simple interpretation in this model. As discussed above, the irreversible coupling of high-lying collective mode (representing the GDR) to the low-lying configuration (appearing at $T \neq 0$) leads to the energy dissipation of the former to the latter. This dissipation, on the one hand, increases the damping, on the other hand reduces the strength of the high-lying peak, conserving the total integrated dipole strength [the energy-weighted sum rule (EWSR)] in the whole energy interval $0 < \eta < 20$ MeV. The competition of these two effects leads to the saturation of the GDR thermal damping width at a certain temperature T. At $T \geqslant 4-6$ MeV the GDR is hard to be seen as its strength is almost absorbed by the low-lying mode. Obviously the EWSR is conserved only for the total system ($0 < \eta < 20$ MeV), while it decreases as increasing T in the collective subspace, corresponding to the GDR peak ($11 < \eta < 20$ MeV). This feature is a natural consequence whenever a close system is decomposed into two (well-separated and open-to-each other) relevant and irrelevant subsystems, which in the present case consist of the collective ph excitations and the noncollective pp and hh configurations, constituting the heat bath, respectively. The irreversible coupling of relevant subsystem (the hot GDR) to the irrelevant one (the heat bath) leads to an energy flow from the former to the later. The loss of collectivity, reported by Gaardhoje [2], and the disappearance of the hot GDR, observed in the experiments at high temperatures (see, e.g., Ref. [38]), can be therefore interpreted within our approach as the result of a complete dissipation of the collective ph modes to the noncollective degrees of freedom in the heat bath. Physically this means that as the temperature increases, the possibility for the development of pure quantal collective excitations, such as the coherent motion of *all* protons against *all* neutrons in phase, is reduced to vanish completely at $T \sim 5-6$ MeV because of the increase of stochastic motion of noncollective degrees of freedom constituting the heat bath.

It is exciting that Ref. [28] (see also [29]), which approached the damping mechanism using the linear response theory, has exposed a quite similar feature. Here one observes that the strength of the high-lying resonance is transferred to a pronounced low-lying mode (or moved gradually to the low energy region) in such a way that it ceased to exist at around $T = 3$ MeV since the low frequency mode has exhausted all the strength. It is worth noticing that the effects of the residual interaction was taken into account in Refs. [28,29] by dressing the particles and holes such as to create an imaginary part of their self-energies. This scenario can be compatible with the present approach, which leads to the polarization operator, whose imaginary part yields the thermal damping. Clearly, the imaginary part of the self-energy, which was taken as an ansatz in Ref. [28] may contain also the effects of $2p2h$ configuration mixing as well. Even though starting from a different approach, Refs. [28,29] came to a similar conclusion regarding the damping at finite temperature. Indeed, the damping factor in Ref. [29] is proportional to the friction coefficient divided by the square root of the local stiffness, which also reach a plateau at $T \sim 3-4$ MeV. In order to see the correspondence between our approach and the one in Refs. [28,29] it is necessary to establish a clear relation between the imaginary part in Eq. (3) of Ref. [28] and the thermal damping and spreading widths of GDR discussed in the previous sections. There is

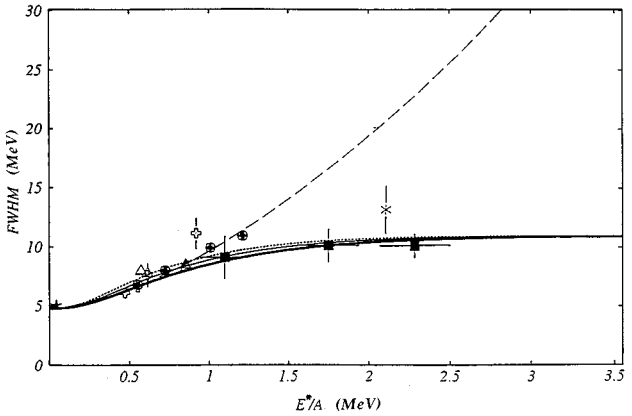

FIG. 6. FWHM of the GDR as a function of the excitation energy per nucleon $E^*/A \equiv aT^2/A$. The results obtained within our formalism are shown by the thick ($a=A/8$), thin ($a=A/9$), and dotted ($a=A/10$) curves. The dashed curve represents $\Gamma = 4.8[1+(E^*/A)^{1.6}]$ [3]. Data are from Refs. [2] (white crosses), [3] ($\odot$), [4] ($\triangle$), [5] (*), [6] (black $\square$), [7] ($\bullet$), and [37] ($\star$).

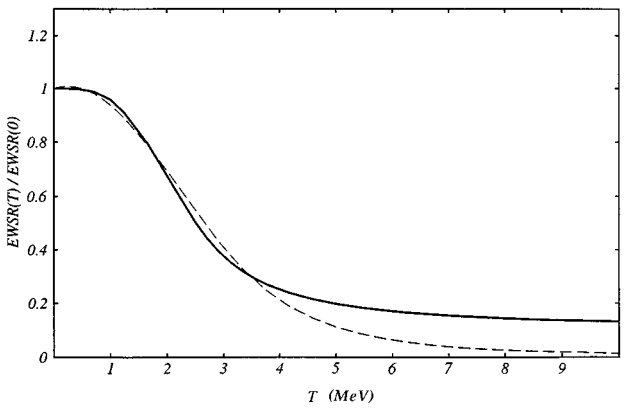

FIG. 7. The ratio EWSR(T)/EWSR(0) as a function of temperature. The solid curve is obtained by using the width $\Gamma_\mu = \Gamma_\mu^{\rm ITD}$ within our formalism, while the dashed curve has been calculated with $\Gamma_\mu \equiv \Gamma - \Gamma_Q \equiv 4.8(E^*/A)^{1.6}$ from Ref. [3] and using the level-density parameter $a=A/8$.

no doubt that this would be a formidable task, which, once completed, would resolve the long-standing discrepancies between several existing approaches to the hot GDR puzzle.

The total GDR width Γ (FWHM), which combines both the quantal spreading width $\Gamma^{\downarrow}$ and the integrated thermal damping one $\Gamma_\mu^{\rm ITD}$, is calculated from Eqs. (3.4) and (3.5). Hereafter we suppose that the quantal width Γ_Q can be described within the framework of a microscopic approach, such as in Refs. [23]. The GDR in cold nuclei can then be approximated by a single collective excitation, whose strength has a Lorenzian distribution centered at the GDR energy centroid $\overline{E}$ with the FWHM equal to the quantal spreading width $\Gamma^{\downarrow}$. Following the calculations in Refs. [22,23], we can put $\Gamma_Q = \Gamma^{\downarrow} =$ 4.8 MeV [37] independently of temperature. The initial values for the width Γ of the GDR and the energy shift δE [Eqs. (3.7) and (3.8)] turn out to be very close to the exact ones in the present case. This provides a convergence of the iteration procedure with a good precision (<1 keV) already at the second step in solving Eqs. (3.4) and (3.5). The result for the FWHM of the GDR centered at $E=\overline{E}_{\rm GDR}$ is plotted versus the excitation energy per nucleon in Fig. 6, where the experimental systematic for Sn isotopes [2–7] are also collected. In converting temperature to the excitation energy $E^*=aT^2$, we used several values for the level density parameter $a=A/8-A/10$. It is seen from Fig. 6 that the qualitative behavior of the GDR width observed in the experiments is well reproduced by applying our formalism to the simple model. The closest curve to the experimental systematic is obtained by using the level-density parameter $a=A/8$ and $A/9$. The total GDR width increases strongly as a function of the excitation energy up to $E^*/A \sim 1.1-1.2$ MeV corresponding to $E^* \sim$ 120 – 130 MeV and thereafter becomes approximately constant. We would like to emphasize only on the qualitative side of the present schematic calculations. In fact the pretty good agreement with the experimental systematics shown in Fig. 6 may be illusory, since one should not forget that we have used the same matrix element and interaction parameter k for all ph as well as pp and hh configurations. Reducing, e.g., the interaction parameter k for pp and hh levels, the saturated value of the GDR width above $E^*/A \sim 1.1-1.2$ MeV becomes lower accordingly. Other mechanisms such as shape fluctuations, etc., also contribute to the total width. In the present schematic estimation these effects are effectively included owing to a large smearing parameter $\varepsilon = 1$ MeV. This feature also agrees with the observation in Ref. [27]. The thermal damping width also depends on the distant between shells, which is kept equal to 6 MeV in the present calculations. With Fig. 6 we would like just to point out that the saturation behavior of the GDR width can be understood in the present formalism.

We finish the present section with a discussion on the *limiting temperature*, above which the GDR does not exist [38]. In this respect our formalism gives a different mechanism from the classical approach in Ref. [39], where the conclusion about the disappearance of the GDR came from its exceedingly large width at high temperature. In fact, the GDR width in our model remains nearly constant at excitation energy $E^* > 130$ MeV. The saturation of the GDR width is not the real signature for its disappearance at high temperatures. In the region with saturated width, the limiting temperature for the GDR can be discussed by using the integrated energy weighted strength. The EWSR of the GDR decreases as increasing temperature at least in the present schematic model because of the existence of the low-lying mode (Fig. 4). The ratio EWSR(T)/EWSR(0) over the energy interval of the GDR localization in the present model is shown in Fig. 7 (solid curve). The EWSR obtained by using the width given by the fit $\Gamma - \Gamma_0 = \Gamma_0 (E^*/A)^{1.6}$ [3] is also shown by the dashed curve. The saturation temperature can be defined as $T \sim 3.5$ MeV corresponding to the point where the two curves start to deviate. However the EWSR becomes really small ($<10\%$ of the ground state GDR EWSR) at higher temperature around ~ 5 MeV. Therefore it may be a good reason to consider the temperature T around 5 MeV as the limiting temperature for the existence of the GDR in hot nuclei.

V. CONCLUSIONS

We have presented an approach, which allows to derive *the thermal damping width* of the GDR in hot nuclei in a

microscopic way. We have demonstrated the importance of the thermodynamical effects in the noncollective pp and hh configurations, which appear only at nonzero temperature and can play the role of a background or the heat bath. Namely, we have pointed out that the irreversible coupling of the ph GDR to this background (or heat bath) leads to the thermal damping of GDR in hot nuclei. The application of our approach to a simple schematic model has shown that this thermal damping mechanism can be complementary to other mechanisms in understanding the behavior of the GDR width at finite temperature. Finally a semimicroscopic unification of the *quantal spreading* and the *integrated thermal damping widths* shows that the behavior of the total width found in this approach is similar to the tendency in the experimental findings in hot Sn isotopes including the region of width saturation. Our analysis has been performed within an oversimplified schematic model. A drawback of this model is, while the GDR can be described by one single collective ph transition, the degeneracy of noncollective pp and hh configurations on only two levels made them too collective and therefore artificially enhanced intensity of the low lying mode. In realistic situations we expect that a very large number of noncollective pp and hh degrees of freedom will spread out the strength distributed on them. In our opinion, the difference between the present schematic model and the reality is the difficulty of separating the low-lying modes out from the background in realistic situations. Therefore in reality high-precision measurements are required in the low-energy part of the γ-decay spectrum of hot nuclei. Nonetheless, since the mechanism of the thermal damping arises from the coupling between collective and noncollective degrees of freedom, we believe that the qualitative conclusion of our formalism on the behavior of the hot GDR, including the region of width saturation, is model independent.

ACKNOWLEDGMENTS

The authors are grateful to K. Kumar for fruitful discussions. N.D.D. acknowledges with thanks the support from the Nishina Memorial Foundation and the Science and Technology Agency of Japan, under which this work was done.

APPENDIX: PHYSICAL MEANING OF POLARIZATION OPERATOR IN THE EXAMPLE OF DAMPED HARMONIC OSCILLATOR

Let us consider a simple example of an ideal harmonic oscillator R coupled to a heat bath I. The Hamiltonian of the free oscillator is

$$H_R=\omega Q^\dagger Q, \tag{A1}$$

where the ideal boson operators $Q^\dagger$ and Q create and annihilate, respectively, an elementary excitation (quanta) of energy ω in the oscillator. The free heat bath Hamiltonian need not be specified in the present example. The oscillator heath bath coupling is chosen as

$$H_{RI}=g(QB^\dagger+Q^\dagger B), \tag{A2}$$

with unspecified dimensionless heat bath operators $B^\dagger$ and B.

The two-time Green's functions $G(t-t')$ and $\Gamma(t-t')$, which describe the motion of the oscillator in the heat bath, and the influence of the heat bath respectively, are defined similarly to Eqs. (2.19) and (2.20). Applying the two-time Green's function method in the same way as in Sec. II, we get the corresponding set of equations for these two-time Green's functions

$$i\frac{\partial}{\partial t}G(t-t')=\delta(t-t')+\omega G(t-t')+g\Gamma(t-t'), \tag{A3}$$

$$i\frac{\partial}{\partial t}\Gamma(t-t')=NgG(t-t'). \tag{A4}$$

Their Fourier images satisfy the equations

$$\eta G(\eta)=\frac{1}{2\pi}+\omega G(\eta)+g\Gamma(\eta), \tag{A5}$$

$$\eta\Gamma(\eta)=NgG(\eta). \tag{A6}$$

Equation (A4) is derived as a result of decoupling similar to Eq. (2.23)

$$\begin{aligned}&\langle\langle[B(t),B^\dagger(t')]Q(t);Q^\dagger(t')\rangle\rangle\\&\quad\approx\langle[B(t),B^\dagger(t)]\rangle\langle\langle Q(t);Q^\dagger(t')\rangle\rangle\\&\quad=\langle[B(t),B^\dagger(t)]\rangle G(t-t')\equiv NG(t-t').\end{aligned} \tag{A7}$$

Eliminating function $\Gamma(\eta)$ by expressing it in terms of $G(\eta)$ from Eq. (A6) and substituting the result for Eq. (A5) finally leads to an equation for the Green's function of the oscillator

$$[\eta-\omega-P(\eta)]G(\eta)=\frac{1}{2\pi}, \tag{A8}$$

where the polarization operator $P(\eta)$ in this example is

$$P(\eta)=\frac{N}{\eta}g^2. \tag{A9}$$

Converting the last term on the RHS of Eq. (A3) in term of its Fourier transform $\Gamma(E)$ $(E=\eta+i\varepsilon)$ and using Eqs. (A6) and (A9) to express $\Gamma(E)$ in terms of $G(E)$ and $P(E)$, we get

$$\begin{aligned}i\frac{\partial}{\partial t}G(t-t')&=\delta(t-t')+\omega G(t-t')\\&\quad+\int_{-\infty}^{\infty}P(\eta+i\varepsilon)G(\eta+i\varepsilon)\\&\quad\times e^{-i\eta(t-t')+\varepsilon(t-t')}d\eta.\end{aligned} \tag{A10}$$

If the main value of the function $P(E)$ comes around the pole η of Eq. (A8) we can take $P(E)$ out of the integral, approximating $P(\eta+i\varepsilon)\equiv\mathrm{Re}[P(\eta+i\varepsilon)]+\mathrm{Im}[P(\eta+i\varepsilon)]$ by its value around the pole. The remaining integral is noth-

ing but the double-time Green's function $G(t-t')$ thanks to its analytical property. We end up with

$$\frac{\partial}{\partial t}G(t-t')=[-i(\omega+\Delta)+\gamma]G(t-t'), \quad t\neq t' \tag{A11}$$

where

$$\Delta=\mathcal{P}\mathrm{Re}[P(E)]_{E=\eta+i\varepsilon}=\mathcal{P}\frac{N}{\eta}g^2,$$

$$\gamma=\mathrm{Im}[P(E)]_{E=\eta+i\varepsilon}=\pi N g^2\delta(\eta).$$

It is easy to recognize that Eq. (A11) is nothing but the equation for the damping of the harmonic oscillator, where Δ is the energy shift and γ is the damping coefficient.

[1] *Proceedings of the Gull Lake Nuclear Physics Conference on Giant Resonances*, edited by M. Thoennessen [Nucl. Phys. **A569** (1994)].

[2] J. J. Gaardhøje *et al.*, Phys. Lett. **139B**, 273 (1984); J. J. Gaardhøje *et al.*, Phys. Rev. Lett. **53**, 148 (1984); J. J. Gaardhøje, A. M. Bruce, and B. Herskin, Nucl. Phys. **A482**, 121c (1988); C. A. Gossett *et al.*, Phys. Rev. Lett. **54**, 1486 (1985).

[3] D. R. Chakrabarty *et al.*, Phys. Rev. C **36**, 1886 (1987); D. R. Chakrabarty, Nucl. Phys. **A382**, 81c (1988).

[4] R. J. Vojtech *et al.*, Phys. Rev. C **40**, 2441 (1989).

[5] A. Bracco, Phys. Rev. Lett. **62**, 2080 (1989); A. Bracco *et al.*, Nucl. Phys. **A519**, 47c (1990).

[6] G. Enders *et al.*, Phys. Rev. Lett. **69**, 249 (1992).

[7] H. J. Hofmann *et al.*, Nucl. Phys. **A571**, 301 (1994).

[8] J. H. Le Faou *et al.*, Phys. Rev. Lett. **72**, 3321 (1994).

[9] J. L. Egido and P. Ring, J. Phys. G **19**, 1 (1993).

[10] R. A. Broglia, P. F. Bortignon, and A. Bracco, Prog. Part. Nucl. Phys. **28**, 517 (1992).

[11] A. Bonasera, M. Di Toro, A. Smerzi, and D. Brink, Nucl. Phys. **A569**, 215c (1994).

[12] D. Perroutsakou *et al.*, Nucl. Phys. **A600**, 131 (1996).

[13] A. Bracco *et al.*, Nucl. Phys. **A569**, 51c (1994).

[14] M. Mattiuzzi *et al.*, Phys. Lett. B **364**, 13 (1995).

[15] M. Gallardo, M. Diebel, T. Døssing, and R. A. Broglia, Nucl. Phys. **A443**, 415 (1985).

[16] M. Gallardo, F. J. Luis, and R. A. Broglia, Phys. Lett. B **191**, 222 (1987).

[17] N. Dinh Dang, J. Phys. G **16**, 623 (1990).

[18] P. F. Bortignon, A. Bracco, D. Brink, and R. A. Broglia, Phys. Rev. Lett. **67**, 3360 (1991).

[19] H. Sagawa, and G. F. Bertsch, Phys. Lett. **146B**, 138 (1984).

[20] N. Dinh Dang, J. Phys. G **11**, L125 (1985); N. Dinh Dang, and N. Zuy Thang, *ibid.* **14**, 1471 (1988).

[21] N. Dinh Dang, Phys. Rev. C **45**, 1120 (1992).

[22] P. F. Bortignon, R. A. Broglia, G. F. Bertsch, and J. Pacheco, Nucl. Phys. **A460**, 149 (1986).

[23] N. Dinh Dang, Nucl. Phys. **A504**, 143 (1989).

[24] A. V. Ignatyuk, Izv. Akad. Nauk SSSR, Ser. Fiz. **38**, 2613 (1974); A. V. Ignatyuk, *Statistical Properties of Excited Atomic Nuclei* (Energoatomizdat, Moscow, 1983).

[25] M. Sommermann, Ann. Phys. (N.Y.) **151**, 163 (1983).

[26] N. Vinh Mau, Nucl. Phys. **A548**, 381 (1992).

[27] F. L. Braghin and D. Vautherin, Phys. Lett. B **333**, 289 (1994).

[28] H. Hofmann, S. Yamaji, and A. S. Jensen, Phys. Lett. B **286**, 1 (1992); S. Yamaji, A. S. Jensen, and H. Hofmann, Prog. Theor. Phys. **92**, 773 (1994).

[29] S. Yamaji, H. Hofmann, and R. Samhammer, Nucl. Phys. **A475**, 487 (1988).

[30] D. N. Zubarev, Sov. Phys. Usp. **3**, 320 (1960).

[31] V.G. Soloviev, *Theory of Complex Nuclei* (Pergamon, Oxford, 1976); Prog. Part. Nucl. Phys. **19**, 107 (1987); *Theory of Atomic Nuclei—Quasiparticles and Phonons* (Energoatomizdat, Moscow, 1989).

[32] A. Bohr and B. R. Mottelson, *Nuclear Structure* (Benjamin, New York, 1969), Vol. 1, App. 2D, pp. 302–307.

[33] B. Lauritzen, T. Døssing, and R. A. Broglia, Nucl. Phys. **A457**, 61 (1986).

[34] B. Lauritzen, R. A. Broglia, W. E. Ormand, and T. Døssing, Phys. Lett. B **207**, 238 (1988).

[35] J. L. Egido and A. Faessler, Z. Phys. A **339**, 115 (1991).

[36] Ph. Chomaz, Nucl. Phys. **A569**, 203c (1994).

[37] C. T. Kuo, B. S. Ratner, and B. V. Sergeev, Sov. Phys. JETP **13**, 60 (1961); S. C. Fultz *et al.*, Phys. Rev. **186**, 1255 (1969).

[38] K. Yoshida, *et al.*, Phys. Lett. B **245**, 7 (1990); J. Kasagi and K. Yoshida, Nucl. Phys. **A569**, 195c (1994).

[39] A. Smerzi, A. Bonasera, and M. Di Toro, Phys. Rev. C **44**, 1713 (1991); A. Smerzi, M. Di Toro, and D. M. Brink, Phys. Lett. B **320**, 216 (1994).